The Deformable Urinary Tract Phantom: A New Testbed for Urodynamic Ultrasound Studies

Takuro Ishii[1], Hassan Nahas[1], Adrian J.Y. Chee[1], Billy Y.S. Yiu[1], Alfred C.H. Yu[1]
[1]Schlegel-UW Research Institute for Aging, University of Waterloo, Waterloo, ON, Canada

Background, Motivation and Objective

In urology, high-frame-rate ultrasound has demonstrated potential in achieving time-resolved visualization of urine passage (UMB, 2017; 43:2601-10). Such visualization is of practical importance as it can facilitate functional impact analysis of pathological conditions like urethral obstruction. However, validating the efficacy of high-frame-rate urodynamic ultrasound *in vivo* is challenging. It is essential to devise urethra phantoms that can serve as investigative platforms, but existing phantoms are incapable of modeling urethra kinetics during voiding, specifically the urethra's passive deformation from a collapsed state. Here, we present a new deformable urethra phantom design that can simulate the geometric, mechanical and urodynamic characteristics of a male prostatic urethra.

Statement of Contribution/Methods

Each urethra phantom was devised using lost-core molding principles. First, we drafted molds to fabricate walled phantoms of the male prostatic urinary tract with and without 40% benign prostatic hyperplasia (BPH) obstruction, and they were 3-D printed. Next, the urinary tract was constructed using 8% PVA hydrogel. Each model was affixed to a box and the flow channel was collapsed by deflating the urinary tract while an agar-gelatin prostate mimicking slab was casted around the phantom (Fig. b). Lastly, a programmable pump was used to simulate bladder contraction and voiding (7ml/s at max flow rate). A phantom's morphological and urodynamic characteristics were assessed in B-mode imaging and vector projectile imaging (VPI) (UMB, 2014; 40:2295-2309).

Results/Discussion

Images acquired at the phantom's mid-sagittal plane showed that the initially-collapsed urinary tract (Fig. c) deformed in response to fluid pressure increase during voiding (Fig. d). The urethra was found to revert to a collapsed state after voiding (Fig. e). During voiding, VPI revealed the presence of flow jet (median velocity: 0.77 m/s; IQR 0.66-0.81 m/s) and turbulence in the BPH-featured model (Fig. f), but these flow features were not observed in the normal model (median velocity: 0.28 m/s; IQR: 0.15-0.43 m/s) (Fig. g). These results indicate that our phantoms can effectively reconstruct urinary fluid-structure interactions during voiding. They serve well as testbeds for the development of urodynamic ultrasound techniques for voiding dysfunction diagnostics.

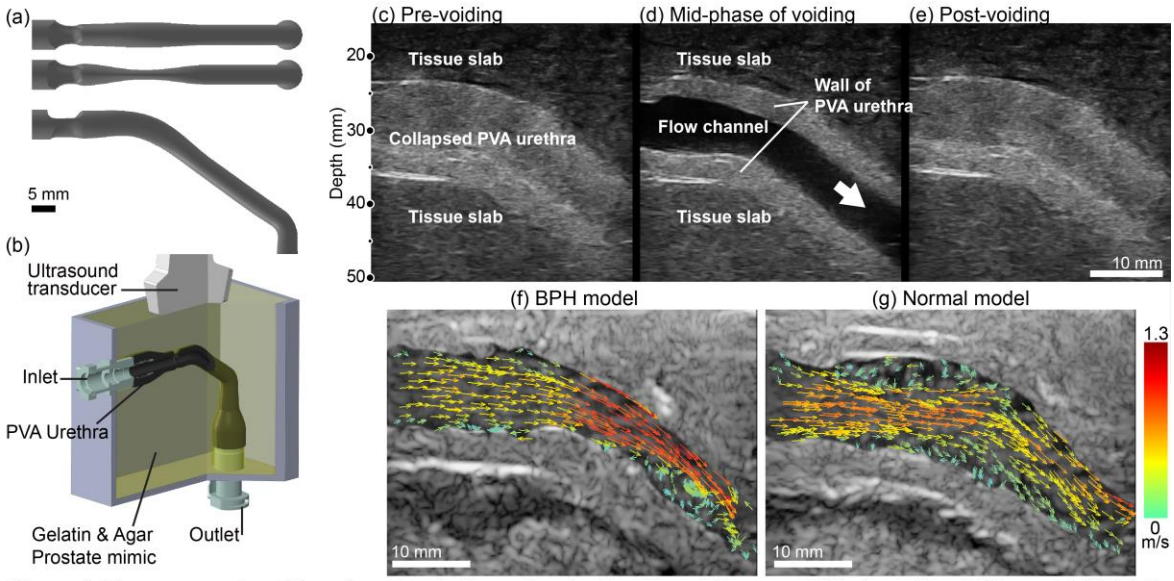

Figure. (a) Inner geometry of the urinary tract. Coronal projection view of the normal (Top), and the BPH model (Middle), and sagittal projection view of both models (Bottom); **(b)** Illustration of the assembly of the deformable urethra phantom; **(c-e)** Mid-sagittal B-mode images of a normal urethra phantom acquired at three time points; **(f,g)** The vector projectile imaging of urinary flow in a BPH and a normal urethra phantom acquired at mid-phase of voiding.